A Peculiar Phase: Heat capacity and Second Sound in Superfluid ^{4}He

Edvin Tewolde Berhane and Brayant Garcia
(Dated: November 17, 2022)

Superfluids are states of matter that have zero viscosity. The superfluid phase of ^{4}He was first discovered in 1937 by Pyotr Kapitsa. Superfluid ^{4}He has the astonishing ability to creep over walls of containers. This is known as film flow and is due to the zero viscosity. In addition, superfluid ^{4}He is the best thermal conductor known. Its high thermal conductivity can be explained through the two-fluid model of superfluid ^{4}He. The two-fluid model also predict propagation of temperature waves in superfluid ^{4}He. Here we measured the speed of temperature propagation and our results are consistent with the two-fluid model. We also measured the specific heat capacity of liquid ^{4}He between $1.73^\circ K$ and $4.00^\circ K$ to observe the superfluid transition. The specific heat capacity showed a discontinuity around $2.17^\circ K$, in accordance with existing literature.

I. INTRODUCTION

The only superfluids which can be studied in the laboratory are the two isotopes of helium: ^{4}He and ^{3}He [1]. Superfluidity was not theorized to exist in ^{4}He before it was discovered in 1937 [2]. Since then, multiple macroscopic and microscopic theories have attempted to explain the phenomena. The defining property of a superfluid is having zero viscosity. It has been experimentally shown that superfluid ^{4}He maintains its flow velocity for long times within a closed loop [3].

Superfluid ^{4}He also exhibits a phenomena known as the fountain effect. A sketch is provided in figure 1. In order to produce this phenomena, a container is partially submerged in superfluid helium. The bottom of the container is a porous plug: a plug that only allows the superfluid component to flow through. When the helium inside the container is heated, the superfluid component outside flows through the bottom of the container to reestablish thermal equilibrium. This increases the pressure inside the container and helium shoots out the top as a result. We observed this phenomena ourselves as a curiosity.

The specific heat capacity of ^{4}He has been shown to diverge around the transition to superfluid phase [4]. Here we measured the specific heat capacity of liquid ^{4}He to check for the divergence indicative of the phase transition. Our results are show a discontinuity near $2.17^\circ K$, consistent with existing literature.

In the superfluid phase, ^{4}He is predicted to support propagation of temperature waves [5]. These temperature waves are known as second sound. The presence of second sound can explain the high thermal conductivity of superfluid ^{4}He. To test the existence of second sound, we measured the speed of temperature propagation in superfluid ^{4}He between $1.76^\circ K$ and $2.17^\circ K$ and compared multiple models for our data. Linear models show the lowest χ^2 on average, indicating the existence of second sound. Our data in figure 7 follows the trend predicted by Landau in [5], but there are significant deviations at multiple temperatures .

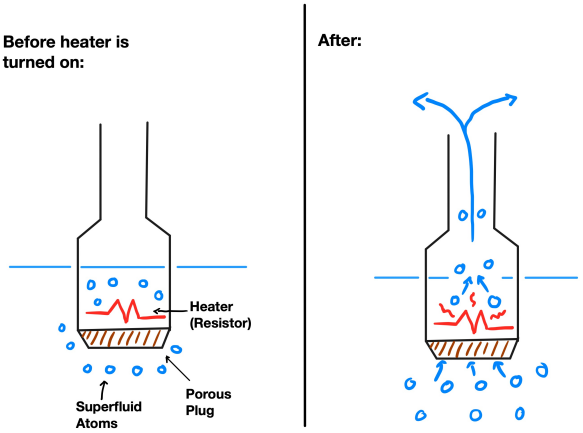

FIG. 1. A sketch to describe the fountain effect. In our observation of the fountain effect, we used a resistor as a heater. After heat is transferred to superfluid helium in the container, a buildup of pressure forces the helium to flow out through the top of the fountain. In turn, superfluid helium outside the container can flow through the porous plug and continue the cycle until thermal equilibrium is re-established.

II. BOSE-EINSTEIN CONDENSATION IN ^{4}HE

Helium is unique in remaining in the liquid phase down to the lowest temperatures measured at one atmosphere [1]. The reason for helium remaining liquid is the low atomic mass and weak interatomic interactions. Since helium remains liquid even at very low temperatures, quantum effects, which only become significant at low temperatures, influence the properties of liquid helium [1]. ^{4}He is a composite boson - it consists of 2 protons, 2 neutrons, and 2 electrons - and can thus be described quantum mechanically using Bose-Einstein statistics.

Satyendra Bose and Albert Einstein developed a theory of ideal boson gases in the early 1900s [6, 7]. An ideal boson gas is a theoretical gas composed of randomly moving one dimensional bosons that are not subject to interparticle interactions. The theory predicts the average number of particles in an ideal boson gas occupying

a quantum state with energy ϵ_k as a function of temperature and chemical potential. Below certain transition temperature T_c, their theory predicts a macroscopic fraction of all particles will be in the $\epsilon_k = 0$ state. Analyzing the theorized heat capacity of an ideal boson gas shows a cusp at this transition temperature T_c, implying a thermodynamic phase transition. Occupation of the zero momentum state χ is the order parameter of this transition. χ is predicted by the theory to increase continuously as the temperature drops below T_c. A continuous order parameter implies a second order phase transition. Second order phase transitions are accompanied by a divergence in specific heat capacity [1]. The state of matter below T_c where a macroscopic fraction of particles are in the zero momentum state is known as a Bose-Einstein condensate.

Below T_c, the particle density n of an ideal boson gas can be split up into a condensate density n_0 and a normal density n_n:

$$n = n_0 + n_n \tag{1}$$

In an ideal boson gas, the condensate density n_0 approaches n as the temperature approaches 0 K. Liquid ^{4}He is however not an ideal boson gas. In liquid ^{4}He, there are significant interactions between atoms. These interactions deplete the fraction of particles in the condensate. Theories attempting to take interactions into account and experiments aimed at measuring the condensate fraction in liquid ^{4}He predict $n_0 \approx 10\%$ at 0 K [8].

III. SUPERFLUIDITY IN ^{4}HE

A superfluid is defined as a fluid with zero viscosity. In 1937, Pyotr Kapitsa found ^{4}He to be a superfluid at low temperatures [2]. The density ρ of superfluid ^{4}He can be modeled as the sum of a superfluid density ρ_s and a normal density ρ_n:

$$\rho = \rho_s + \rho_n \tag{2}$$

This is known as the two-fluid model and was first proposed by Tisza in 1938 [9, 10]. It's important to note that ρ_s does not correspond to n_0. The superfluid fraction ρ_s is defined as the fraction that flows without viscosity and can be larger than the condensate density. Andronikashvili measured ρ_s as a function of temperature experimentally and found the relation showed in figure 2 [11].

Landau expanded on the two-fluid model in his 1941 paper with a complete system of two-fluid hydrodynamic equations [5]. The two-fluid hydrodynamic equations proposed by Landau predict that both normal sound and and second sound waves can travel in superfluid ^{4}He. Landau found the wave speeds to be:

$$u_1 = \left(\frac{dP}{d\rho}\right)^{\frac{1}{2}} \qquad u_2 = \left(\frac{TS^2\rho_s}{C\rho_n}\right)^{\frac{1}{2}} \tag{3}$$

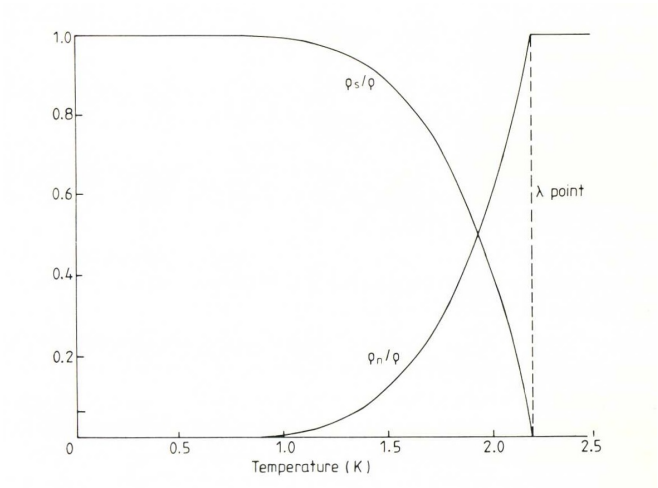

FIG. 2. Andronikashvili's measurement of ρ_s and ρ_n as functions of temperature. At the λ-point, almost all of the helium is in the normal density ρ_n. At around 1K, almost all of the helium is in the superfluid state ρ_s. [11]

where u_1 is the speed of normal sound, P denotes pressure, T is temperature, S is entropy, C is heat capacity, and u_2 is speed of second sound. In normal sound, the total density fluctuates while the ratio of superfluid to normal density stays constant. In second sound, the total density of the fluid is constant while the ratio between the superfluid and normal density fluctuates. Second sound results in temperature propagation because the two components have different temperatures. Temperature usually spreads diffusely through a medium. Wave propagation differs from diffusive propagation in the relationship between distance and time. Distance traveled by a wave is proportional to time, whereas diffusive distance is proportional to the square root of time.

IV. MEASUREMENT OF SPECIFIC HEAT CAPACITY IN ^{4}HE

The specific heat capacity of liquid helium is expected to diverge around the temperature where the transition to superfluid occurs. By accurately measuring specific heat capacity, we can thus determine the transition temperature. Specific heat capacity of a substance, commonly denoted by c, is defined as:

$$c = \frac{1}{m}\frac{\mathrm{d}Q}{\mathrm{d}T} \tag{4}$$

where m is the mass of substance measured and $\mathrm{d}Q$ represents the amount of heat needed to raise the temperature of the sample by an amount $\mathrm{d}T$. Specific heat capacity can vary significantly with temperature and pressure. Here we measured specific heat capacity as a function of temperature.

To measure the specific heat capacity, we used the setup in figure 3. The cell in figure 3 is a copper container.

Our measurements were made on helium inside the cell. To measure specific heat capacity of helium inside the cell, we needed a way to dissipate controlled amounts of heat and measure the temperature change. Heat dissipation was made possible by wrapping a resistance wire around the cell. Temperature measurements were made through germanium resistor attached to the outside of the cell. We refer to the cell, resistance wire, and germanium resistor as the addendum. Germanium has a highly temperature dependent resistance in our temperature interval, but must be calibrated before use.

We calibrated the germanium resistor it using Wallace & Tiernan absolute-pressure gauges and the 1958 ^{4}He scale of temperatures [12]. We used a four-probe technique to measure the resistance of the germanium resistor at multiple temperatures between $1.5°K$ and $4.2°K$. A function of the form:

$$R = \sum_{n=0}^{8} A_n \log^n(T) \tag{5}$$

where R is the resistance and T is the temperature was used to interpolate between the measurements. This type of function is commonly used to calibrate germanium resistors [13, 14]. A plot of the fit to the measured values can be found in the SI.

With the thermometer calibrated, we put a known amount of helium into the capillary leading to the cell. We then cooled the entire setup down to $1.7°K$ by pumping on the liquid helium in the reservoir. During the cooling, the cell was in thermal contact with the liquid helium in the reservoir through helium transfer gas in the IVC. As a result of cooling the cell, the helium gas we put in the capillary was pumped into the cell and liquified. Once $1.7°K$ had been reached, we thermally isolated the cell with liquid helium inside using the sorbtion pump. The sorbtion pump was made by covering a copper plate with charcoal and attaching a diode and a resistor. When charcoal cools down, it adsorbs helium gas. A current through the resistor was used to raise the temperature of the charcoal and release the adsorbed helium. The copper plate was in thermal contact with the inner chamber to cool the charcoal back down once we stopped the current through the resistor. The diode in the pump was calibrated as a thermometer to show when the pump was active. The reason to use the sorbtion pump instead of pumping through the pump tube is speed. To minimize heat leaks, the pump tube is long and narrow. Removing the amount of helium gas necessary to thermally isolate the addendum through the pump tube would take significantly longer than using the sorbtion pump. Good thermal isolation of the addendum is important to ensure all the energy dissipated by the resistance wires heats the cell and not anything else.

To raise the temperature of the thermally isolated addendum, a voltage V was applied to its resistance wire. Let R be the resistance of the wire and Δt the duration of the voltage pulse. The heat ΔQ dissipated by the wire is then given by:

$$\Delta Q = \frac{V^2}{R}\Delta t \tag{6}$$

The heat capacity of the addendum C_{ad} and of the helium inside C_{He} can be found by measuring the temperature change ΔT caused by the heat dissipation. We let the temperature equilibrate and recorded the change through the calibrated germanium resistor:

$$C_{ad} + C_{He} \approx \frac{\Delta Q}{\Delta T} \tag{7}$$

This is an approximation because heat capacity is defined as the limit $\Delta T \to 0$. We ensured the temperature changes were small to get accurate estimates. The heat capacity of our helium sample C_{He} is then found by subtracting the heat capacity of the empty addendum C_{ad} from the right hand side ratio:

$$C_{He} = \frac{\Delta Q}{\Delta T} - C_{ad} \tag{8}$$

We measured the heat capacity of the empty addendum separately using the same procedure as above but without loading helium into the cell. The specific heat capacity of helium c follows from 8 by dividing C_{He} with the mass of helium loaded into the cell m:

$$c = \frac{C_{He}}{m} \tag{9}$$

We calculated m by measuring the pressure change ΔP in a known volume V of pure helium gas at room temperature T and applying the ideal gas law:

$$m = M * \frac{V\Delta P}{RT} \tag{10}$$

where M is the molar mass of helium and R is the ideal gas constant. In our calculation, we assumed that all the helium that left the known volume entered the cell.

V. SPECIFIC HEAT CAPACITY RESULTS

Figure 4 shows our measurements of the specific heat capacity of liquid ^{4}He. The specific heat capacity has a discontinuity at $T_c = 2.1786K$. Around this point, the measurements take a shape resembling the Greek letter λ. Because of this, the point is commonly referred to as the λ-point. Our estimate of the λ-point temperature is based on the temperature where we measured the largest specific heat capacity: $2.1786°K$. The 1958 ^{4}He Scale of Temperatures puts the λ-point at $2.1720°K$ [12].

This deviation could potentially come from an imperfect thermometer calibration. The difference in voltage across the germanium resistor for the $1\,\mu A$ current we used is large enough to be detected: between

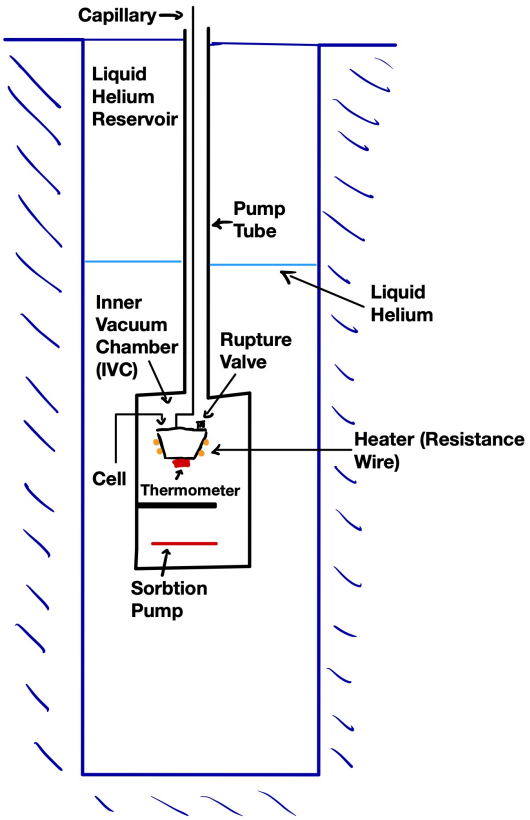

FIG. 3. Schematic of setup for measuring the specific heat capacity of liquid ^{4}He. Wires to the thermometer, resistance wire, and sorbption pump are not shown.

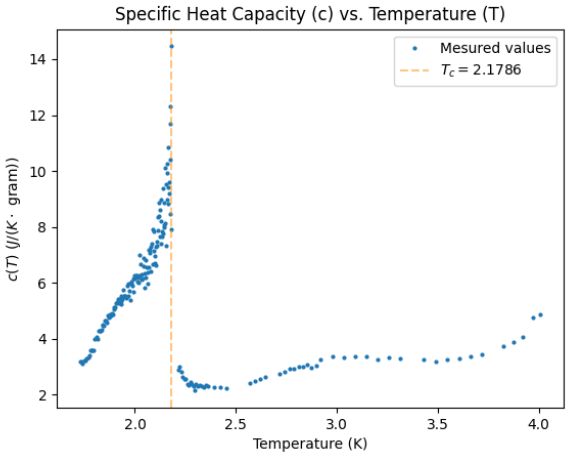

FIG. 4. Measured values for specific heat capacity of liquid ^{4}He. The orange line indicates the temperature at which the highest heat capacity was measured.

$T = 2.1786°K$ and $T = 2.1720°K$, the expected voltage change across the resistor is 0.02844 mV. The difference in vapor pressure could however have been difficult for us to detect. The vapor pressure of ^{4}He at $2.1720°K$ is 37800 microns mercury. At $2.1786°K$, the vapor pressure is 38409 microns mercury [12]. The discrepancy of 409 microns mercury could be caused by human error when reading our analog pressure gauge or inaccuracies in the pressure gauge itself. The Wallace & Tiernan pressure gauge has 1 mm spaced lines every 1000 microns mercury. A small inaccuracy there could cause incorrect pressure readings similar in magnitude to the discrepancy. Incorrect pressure readings would calibrate our germanium resistor incorrectly, which would in turn cause inaccuracies in our temperature values.

VI. MEASURING THE SPEED OF SECOND SOUND

To measure the speed of second sound in superfluid helium, we used the setup shown in figure 6. Second sound is both produced and detected by resistive elements. The pulse source is a 10 Ω nichrome ribbon formed into planar heater. The pulse detector is a bolometer. The bolometer used is a carbon resistor with phenolic insulation removed on one side. The insulation is removed to put the carbon in better thermal contact with the helium and provide shorter response time. In making the measurements, we applied a voltage pulse to the nichrome ribbon to increase the temperature locally and measured the time until a temperature change was recorded by the bolometer.

The time measurement was done using an oscilloscope connected to both the bolometer and the function generator supplying the voltage pulse. A screenshot of the oscilloscope after a measurement is presented in figure 5. The signal from the bolometer had a peak followed by a valley. We recorded the time difference between the peak voltage across the bolometer and the voltage pulse as the time taken for the temperature rise to reach the bolometer. The width of the peak was used as our uncertainty. The valley after the peak indicates the temperature rise is followed by a temperature dip. We saw this consistently on every measurement but are unable to explain why it happens.

To get a better estimate for the propagation speed at each temperature, we measured the time at multiple distances. The distance was adjusted manually from outside the cryostat and measured using a ruler. For each temperature, we measured the time at 4 distances. The rate of propagation was found by fitting a model to our data points.

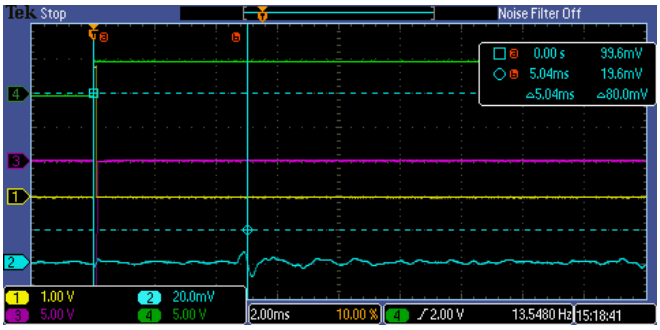

FIG. 5. Screenshot from oscilloscope after second sound measurement. The pulse from the function generator is on channel 1 and the voltage across the bolometer is on channel 2. The change in voltage across the bolometer resulting from the temperature change is marked with blue line b.

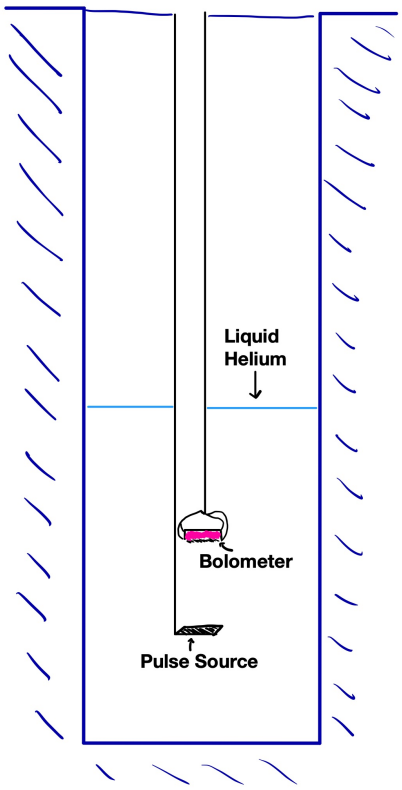

FIG. 6. Schematic of setup for measuring the speed of temperature propagation in superfluid helium. To vary the distance between the pulse source and the bolometer, the bolometer was manually controlled outside the chamber.

VII. SECOND SOUND RESULTS

To test the two-fluid model, we fit both linear and square root models to our data at each temperature. See supplementary material for our data and model fits at each temperature. For each temperature, we had $N = 4$ measurements. The χ^2 values of our square-root model ranged between 40 and 225. Since $\chi^2 > 10N$ for all temperatures, we can rule out the square root model with high certainty. With a constant term, the χ^2 for the square root fit improved to around order $2N$. However, the constant term is always negative and often quite large, indicating temperature diffusion starts multiple milliseconds before we provide our voltage pulse to the planar heater. We believe this is a case of over fitting a 2 parameter model to our 4 data points.

At each temperature, we found that the relation between distance and time was better described by a linear model. Our linear models without a constant term had χ^2 between 9 and 16. This is still larger than our number of data points 4, but significantly better than the square root model without a constant term. With a constant term, the χ^2 for the linear model only went above 2 for our measurement at 2.17 K. Measuring very close to the lambda point brings additional uncertainty as the speed can change very quickly with small changes in temperature. We believe this to be the causing the bad fit at 2.17 K. A constant term in the model can be motivated by delays in the response time for the planar heater and the bolometer, as well as uncertainty in the exact position of the wave.

More data points are needed to further evaluate the linear model, but the results are promising. We are able to rule out the square root model with high certainty based on this measurement but the linear model still stands. The accuracy of the linear model indicates that temperature propagates in superfluid helium like a wave, as predicted by the two-fluid model. The speed at each temperature was taken as the slope of our linear model fit and the results are displayed in figure 7.

We observed a significant decrease in propagation speed as temperature got closer to the λ-point. The decrease in propagation speed close to the λ-point is consistent with the two-fluid model. The two-fluid model predicts the speed u_2 defined in equation 3. As temperature approaches the λ-point, we showed in figure 4 that heat capacity has a sharp increase. In figure 2, it is shown that the fraction ρ_s/ρ_n decreases sharply as temperature approaches the lambda point. We also know the temperature changes between values in figure 7. Entropy will increase as we go up in temperature according to measurements conducted by R. W Hill in 1957 [15]. We plugged these values into the equation for u_2 at the temperatures where we measured second sound and display the results in 7.

Our measured values are higher than u_2 for the higher temperatures, and lower than u_2 for the lower temperatures. The model with a constant term is significantly closer to u_2 for temperatures below 2 K. This could be explained by a non-zero response time in the planar heater and bolometer. A non-zero response time would add a constant time to each measurement, decreasing the velocity unless this constant term is accounted for. At high temperatures, the model without the constant term is

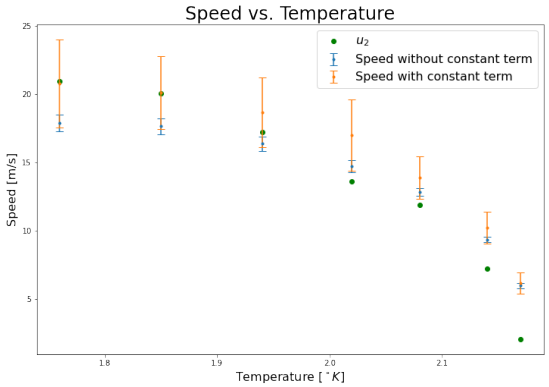

FIG. 7. Speed of second sound plotted against superfluid helium temperature. As helium's temperature increased, the speed of second sound decreased. The lowest speed is approximately $\frac{1}{3}$ of the highest speed.

closer, but none of the models is in strong agreement. This could potentially be caused by the strong dependence of velocity on temperature in this range and inaccuracies in our measurements of temperature through the pressure gauge. This explanation is however not completely satisfactory: the error in the pressure gauge would have to be around 2 mmHg to explain the deviation at the highest temperature, which is more than we are comfortable claiming without additional testing.

VIII. CONCLUSION

Superfluid helium is a fascinating macroscopic exhibit of quantum mechanics. Examining its properties can lead to both new theories and experimental capabilities. For us to get more accurate data on heat capacity, knowing the accuracy of the pressure gauges would have been helpful. We did not perform a calibration of the ones used and don't know their level of accuracy. Greater accuracy in the pressure gauges enables greater accuracy in calibrating the germanium resistor for the heat capacity measurement and more accurate temperature values for our measurement of the speed of second sound. For the second sound measurement, connecting the pressure gauge and pump to the computer and write software to keep the pressure constant would have been helpful. We were keeping the pressure constant by looking at the gauge and manually adjusting the pump valves, but a computer would be more consistent that we could ever hope to be.

To further test the two-fluid model, a natural next step would be to experimentally examine the fraction of superfluid particles ρ_s. This has been done through measuring the inertia of a torsional oscillation of a stack of disks [1]. Combined with a measurement of entropy as made in [15], this would allow to more precisely compare Landau's proposed speed with our measurements.

More data for the speed of second sound at each temperature would enable better comparison between our models and further evaluation of Landau's predicted velocity. We only had 4 data points at each temperature in this experiment. More data would allow us to draw stronger conclusions about the relative accuracy of the models deviations from the predicted velocity.

We would also have liked to measure heat capacity and the speed of second sound at even lower temperatures. As far as we know, there could be additional anomalies in the heat capacity at lower temperatures. Seeing if the speed of second sound continues to be consistent with Landau's proposed formula at lower temperatures would also help further test the accuracy of two-fluid model.

ACKNOWLEDGMENTS

We acknowledge assistance and advice from Professor Amir Yacoby and Professor Isaac F. Silvera on the theory and experimental investigation of superfluid helium. We also acknowledge Joseph Peidle and Jieping Fang for help in understanding the experimental setup and solving any issues that came up. We worked together on the experiments when the measuring of heat capacity. In writing this paper, Edvin extracted the temperature changes for the heat capacity and created figure 4. Edvin also made figures and fit models for the second sound data. Brayant made the schematics of our setups and found the values of u_2. In addition, Brayant wrote the introduction, experimental sections, and appendix. Edvin worked on the abstract, conclusion, results, theory, and experiment sections. We commented on and edited each others writing throughout.

[1] J. F. Annett, *Superconductivity, superfluids and condensates*, Oxford master series in condensed matter physics (Oxford Univ. Press, Oxford, 2004).
[2] S. Balibar, The discovery of superfluidity, J Low Temp Phys **146**, 441– (2007).
[3] W.M. Van Alphen, R. de Bruyn Ouboter, K.W. Taconis, E. van Sprosen, Physica **39**, 109 (1968).
[4] G. Ahlers, Heat capacity near the superfluid transition in he^4 at saturated vapor pressure, Phys. Rev. A **3**, 696 (1971).
[5] L. Landau, Theory of the superfluidity of helium II, Phys. Rev. **60**, 356 (1941).
[6] A. Einstein, Quantentheorie des einatomigen idealen gases. zweite abhandlung, Albert Einstein: Akademie-Vorträge: Sitzungsberichte der Preußischen Akademie der Wissenschaften 1914–1932 , 245 (2005).

[7] A. Einstein, Quantum theory of a monoatomic ideal gas a translation of quantentheorie des einatomigen idealen gases (einstein, 1924) (1925).
[8] D. Tilley and J. Tilley, *Superfluidity and Superconductivity*, Graduate Student Series in Physics (Institute of Physics Publishing, 1990).
[9] L. Tisza, Transport phenomena in helium , Nature **141**, 913 (1938).
[10] L. Tisza, Sur la théorie des liquides quantiques. application a l'hélium liquide, Journal de Physique et le Radium **1**, 164 (1940).
[11] E. L. Andronikashvili, J. Phys. USSR **10** (1946).
[12] H. van Dijk, M. Durieux, J.R. Clement, and J. K. Logan, *The "1958 He^4 Scale of Temperatures" - Tables for the 1958 Temperature Scale* (National Bureau of Standards, 1960).
[13] G. K. White, Experimental techniques in low-temperature physics (Oxford Univ. Press, Oxford, 1987) p. 111.
[14] D. L. Martin, Germanium thermometer calibration, Review of Scientific Instruments **46**, 657 (1975), https://doi.org/10.1063/1.1134283.
[15] R. W. Hill and O. V. Lounasmaa, The specific heat of liquid helium, The Philosophical Magazine: A Journal of Theoretical Experimental and Applied Physics **2**, 143 (1957), https://doi.org/10.1080/14786435708243803.

IX. SUPPLEMENTARY MATERIAL

As described in equation 5, we used a sum of logarithmic powers to model the temperature dependence of our germanium resistor. A plot of the data and our model is shown in figure 8. Plots of our measurements of the speed of second sound and the models we fit to the data are shown in figures 9, 10, 11, 12, 13, 14, and 15.

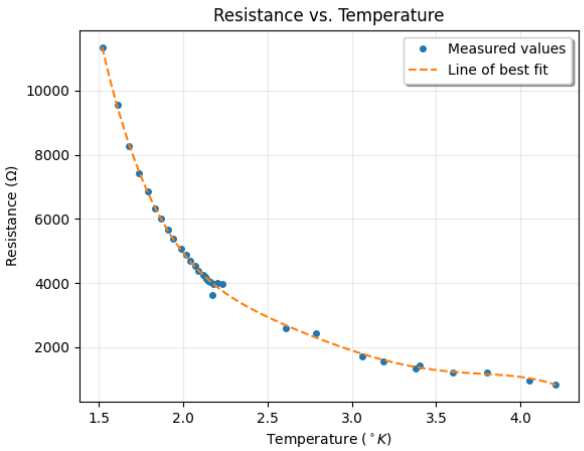

FIG. 8. Model to calibrate germanium resistor

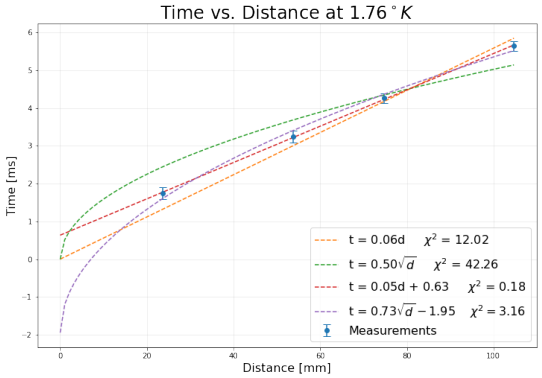

FIG. 9. Measurement of second sound speed at 1.76 K.

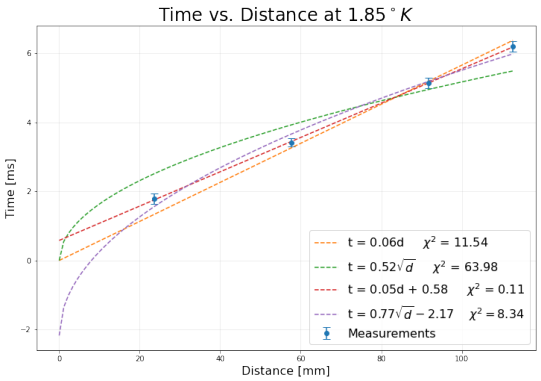

FIG. 10. Measurement of second sound speed at 1.85 K.

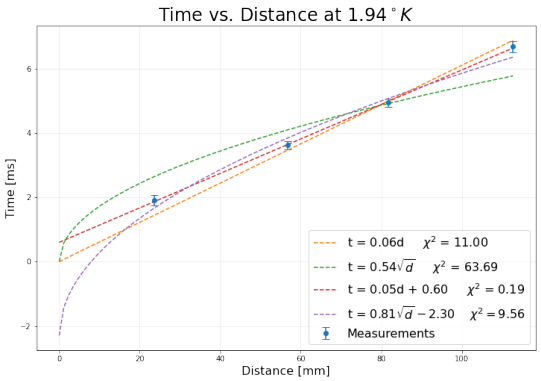

FIG. 11. Measurement of second sound speed at 1.94.

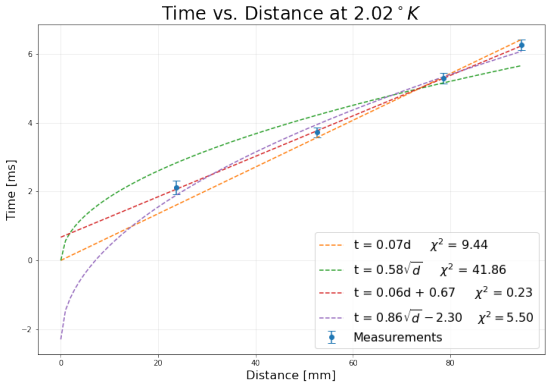

FIG. 12. Measurement of second sound speed at 2.02 K

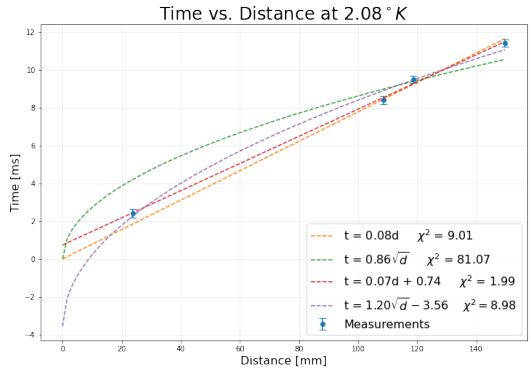

FIG. 13. Measurement of second sound speed at 2.08 K

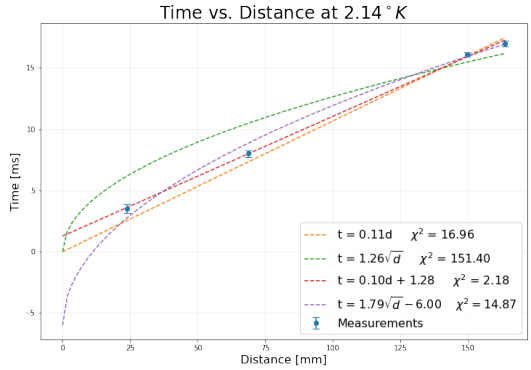

FIG. 14. Measurement of second sound speed at 2.14 K

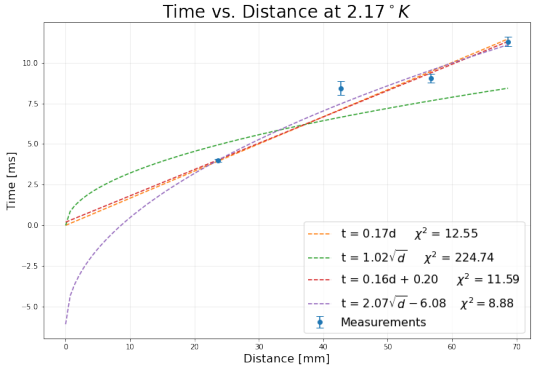

FIG. 15. Measurement of second sound speed at 2.17 K